



EXPLORING THE THERAPEUTIC POTENTIAL OF NATURAL BIOACTIVE COMPOUNDS IN ALK5 INHIBITION FOR NON-SMALL CELL LUNG CANCER (NSCLC) TREATMENT

Rory Anthony Hutagalung^[a,*], Marceline Noviani^[a], Ernawati
Sinaga^[b,*], Rosmalena Rosmalena^[c], Siti Nurbaya^[d], Eldafira Eldafira^[e],
Vivitri Dewi Prasasty^[f,*]

Article History: Received: 10.07.2023

Revised: 01.08.2023

Accepted: 13.08.2023

Abstract

Background: Non-small cell lung cancer, also known as NSCLC, is the type of lung cancer responsible for the biggest number of deaths globally. The signaling protein known as ALK5 plays a significant part in cancer development by contributing to the multiplication of cancer cells and promoting an inflammatory response through its interactions with immune cells. The pharmaceutical industry uses computational ligand-protein docking and screening for various chemicals. This is done to speed up the drug development process and locate promising therapeutic candidates. This research aimed to use computational approaches to search for efficient ALK5 inhibitors that could slow the proliferation of cancer cells. In addition, the research attempted to determine which plant-derived ligand would be the most effective inhibitor by calculating the binding free energy between the ligand and the protein. This would allow for the selection of the most effective plant-derived ligand. **Methods:** In order to achieve this goal, proteins exhibiting a low mutation rate were chosen, and Autodock for Flexible Receptors (ADR) was used to construct the Ramachandran plot, successfully targeting the protein. **Results:** According to the findings of the in-silico research, the molecule farnesiferol c, which is derived from *Ferula assafoetida*, is the most effective ligand to inhibit the ALK5 protein. Its G value is lower than that of commercial medications and 12 other ligands and displays the highest potency level. **Conclusion:** this intriguing chemical is promising as a therapeutic candidate for treating non-small cell lung cancer. However, additional in-vitro testing is necessary to determine that it is effective against the ALK5 protein as a targeted therapy for lung cancer in the future.

Keywords: Non-small cell lung cancer ; ALK5 inhibitor ; Computational docking ; Farnesiferol c

[a]. Faculty of Biotechnology, Atma Jaya Catholic University of Indonesia, Jakarta 12930, Indonesia;

[b]. Faculty of Biology and Agriculture, Universitas Nasional, Jakarta 12520, Indonesia;

[c]. Department of Chemistry, Faculty of Medicine, Universitas Indonesia, Jakarta 10440, Indonesia;

[d]. Department of Clinical Pathology, Faculty of Medicine, Universitas Indonesia, Jakarta 10440, Indonesia;

[e]. Department of Biology, Faculty of Medicine, Universitas Indonesia, Jakarta 10440, Indonesia;

[f]. Department of Pathobiological Sciences, School of Veterinary Medicine, Louisiana State University, Baton Rouge, Louisiana 70803, United States

*Corresponding author: Rory Anthony Hutagalung (email: rory.hutagalung@atmajaya.ac.id) ; Vivitri Dewi Prasasty (email: vprasasty@lsu.edu) ; Ernawati Sinaga (email: ernawatisinagaj@unas.ac.id)

INTRODUCTION

Cancer is a pathological condition characterized by the uncontrolled proliferation of tumor cells. Lung cancer is a leading cause of the most cancer-related deaths worldwide [1]. Lung cancer, as a disease, can be categorized into two main types: non-small cell lung cancer (NSCLC) and small cell lung cancer (SCLC). NSCLC accounts for approximately 85% of all lung malignancies, while SCLC makes up 15% [2]. Non-small cell lung cancer (NSCLC) can be classified into three groups based on cell type and histological classification: large cell cancer, adenocarcinoma, and squamous cell carcinoma. The etiology of lung cancer has been extensively studied concerning various factors, including tobacco smoking [3],

genetic factors [4], diet and obesity [5, 6], and specific environmental factors like air pollution [7, 8]. Common symptoms of lung cancer include weight loss, coughing up blood, chest pain, persistent cough, shortness of breath, wheezing, hoarseness, shoulder pain, and fatigue [9, 10].

Lung cancer is a significant cause of death, and various therapeutic approaches have been implemented to address this issue. The treatment options for lung cancer include surgery, chemotherapy, radiation therapy, combination therapy, and targeted therapy [11]. Chemotherapy involves using a combination of medications, while targeted therapies are specifically designed to attack cancer cells by binding to or blocking targets on the surface of the cells. In certain situations, targeted compounds may not effectively combat

diseases, leading to the possibility of cancer reemerging. Additionally, the drug can have toxic effects on the body and potentially cause severe side effects [12].

Currently, the investigation of structure-based virtual computing is a process that can effectively reduce the time and cost associated with discovering new drugs. In the lungs, epithelial cells, alveolar macrophages, tissue macrophages, and fibroblasts produce TGF- β type 1 (TGF- β 1) or activin-like kinase 5 (ALK5). These cells are exposed to hazardous substances such as silica, bleomycin, and hyperoxia [13].

Recent research has discovered that the tumor suppressor function of TGF- β is lost in the early stages of cancer, similar to the recessive loss of function mutations found in other tumor suppressors [14]. Type 1 TGF- β signaling plays a significant role in cancer formation [15]. It assists cancerous cells in resisting immune cells and increases inflammation [16, 17]. Targeting TGF- β signal transduction in tumors may offer a novel approach to controlling tumor growth by inhibiting its effects. Thirteen ALK5 inhibitor ligands derived from various plant compounds have undergone clinical testing for their potential in treating diseases, including lung cancer. The first ligand is tubulosine, found in *Pogonopus speciosus* (Jack) [18] which can interfere with protein synthesis by inhibiting the process of peptide chain elongation [19]. The second ligand farnesiferol c of *Ferula assafoetida* can inhibit lung cancer cell growth in mice [20]. The third to ninth ligand are isoquinoline alkaloids (chelerythrine, stylopine, sanguinarine, berberine, allocryptopine, coptisine, and protopine) of the family Papaveraceae plants that can inhibit cancer cells [21], genistein is a ligand tenth of *Genista tinctoria* L. to inhibit protein-tyrosine kinase [22], antofine is a ligand eleventh of *Cynanchum paniculatum* Kitagawa which is a protein synthesis inhibitor [23], xanthorrhizol of rhizomes *Curcuma xanthorrhiza* Roxb. which inhibits the growth and development of tumors [24], and lastly, the thirteenth ligand i.e., mimosine of *Leucaena leucocephala* (Lam.) de Wit which inhibits the proliferation of liver cancer cells and lung cancer cells and block the development cycle from the G1 phase to the S phase [25].

Computational ligand-protein docking and screening are extensively utilized in the pharmaceutical industry to expedite drug discovery and identify potential drug candidates from various compounds. Simulating a fully flexible receptor or ligand can enhance the accuracy of binding energy compared to using a rigid receptor or ligand, which has been commonly employed in simulations. Flexibility in intrinsic proteins is often underestimated during the drug discovery process. However, a growing body of evidence indicates that many of the proteins targeted for therapeutic purposes exhibit flexibility. According to previous research [26], the docking attachment protein can perform only 70% of the ligands on average correctly [26]. The percentage experienced a significant increase when the receptor's flexibility in utilizing multiple receptor conformations was considered [27].

This study aimed to use computational methods to screen for effective inhibitors (ligands) of TGF- β receptors, intending to inhibit the growth of cancer cells. Specifically, the study

aimed to identify the best plant-derived ligands as inhibitors of the TGF- β type 1 receptor by estimating the binding energy of the ligand-receptor complex.

MATERIALS AND METHODS

Materials

The receptor complex and its sequence were obtained from the Protein Data Bank Repository with the identifier 5FRI [27]. The corresponding files, in .pdb format, were downloaded (see Appendix 1). Additionally, a 3D file conformer of the commercial drug Carboplatin (ID: 38904) and thirteen ligand files with the following IDs: 639288, 93135, 15559239, 72322, 3862, 72341, 5280961, 2703, 5154, 98570, 4970, 440583, and 2353 were downloaded from PubChem [28]. These ligand files are in .sdf format.

Protein Preparation and Virtual Screening

The protein was prepared, and its mutation rate was assessed using the NCBI BLAST web server [29]. The Pdb files of the protein, after removing the initial ligands and water molecules with Discovery Studio Visualizer (see Appendix 15) [30], were then evaluated using the Ramachandran plot on the RAMPAGE website [31]. To ensure compliance with Lipinski's rules of five, the ligands were screened using the SwissADME website [32].

Molecular Docking

The protein and ligand were prepared using AutoDock Tools [33] software and converted into .pdbqt format, which was necessary for running the AGFR (AutoGrid Flexible Receptors) and ADFR (AutoDock for Flexible Receptors) programs [34]. AGFR and ADFR required the protein and ligand files in this specific format. After running AGFR, it generated an affinity map in .zip format, which will be utilized in the ADFR process.

Protein and Ligand Interaction

The protein and ligand docking data are merged into a unified .pdb file format using PyMOL [35]. Subsequently, this file is edited with Notepad++ [36] to enable the visualization of complex protein and ligand interactions in 2D using LigPlot [37]. Additionally, the interactions can be viewed in 3D using PyMOL.

RESULTS

Protein Identification

The ALK5 protein structure (Figures 1a and 1b) was identified by retrieving its sequence from the Protein Databank Repository in FASTA format. A BLAST similarity search was conducted to assess its similarity to other proteins (Figure 1c). Proteins with a low E-value (0.0) displayed significant similarity to the target sequence, indicating shared structure and function and a low mutation rate.

5FRI:A|PDBID|CHAIN|SEQUENCE
GGTIARTIVLQESIGKGRFGEVWRGKWRGEEVAVKIFSSREERSWFREAEIYQTVMLRH
ENILGFIAADNKDNGTWLWLVSDYHEHGSLFDYLNRYTIVTEGMKLLALSTASGLAH
LHMEIVGTQGKPAIAHRDLKSKNILVKKNGTCCIADLGLAVRHDSATDTIDIAPNHRVG
TKRYMAPEVLDDSDINMKHFESFKRADIYAMGLVFEIARRCSIGGIHEDYQLPYDLPV
SDPSVEEMRKVVCEQKLRPNIPNRWQCEALRVMAKIMRECWYANGAARLTALRIKKT
LSQLSQQ

A



B

Secure | https://blast.ncbi.nlm.nih.gov/Blast.cgi

Blaze Kuliah Universi... Morfologi Koloni dan... Perhitungan Koloni b... Perhitungan Jumlah E... LAPORAN PERHITUN... latihan kesetimban... download.portalge... lib.tenas.ac.id/ks/ep

Sequences producing significant alignments:

Select: All None Selected 0

Alignments | Download | GenPlot | Graphics | Distance tree of results | Multiple alignment

Description	Max score	Total score	Query cover	E value	Ident	Accession
<input type="checkbox"/> PREDICTED: TGF-beta receptor type-1 isoform X2 (Cercopithecus aethiops)	630	630	99%	0.0	100%	XP_011931220.1
<input type="checkbox"/> PREDICTED: TGF-beta receptor type-1 isoform X1 (Papio anubis)	630	630	99%	0.0	100%	XP_009186688.1
<input type="checkbox"/> Chain A, Ah5 in Complex With An N4-(4-aminino-2-spyridyl)acetamide Inhibitor	630	630	100%	0.0	100%	SFR_A
<input type="checkbox"/> PREDICTED: TGF-beta receptor type-1 isoform X1 (Mesocricetus auratus)	630	630	99%	0.0	100%	XP_005078788.2
<input type="checkbox"/> TGF-beta receptor type-1 isoform 1 precursor (Homo sapiens)	630	630	99%	0.0	100%	NP_004603.1
<input type="checkbox"/> PREDICTED: TGF-beta receptor type-1 isoform X1 (Macaca nemestrina)	630	630	99%	0.0	100%	XP_0111731920.1
<input type="checkbox"/> PREDICTED: TGF-beta receptor type-1 isoform X1 (Cercopithecus aethiops)	630	630	99%	0.0	100%	XP_011931220.1
<input type="checkbox"/> PREDICTED: TGF-beta receptor type-1 isoform X1 (Pan troglodytes)	630	630	99%	0.0	100%	XP_009455268.1
<input type="checkbox"/> PREDICTED: TGF-beta receptor type-1 isoform X2 (Callithrix jacchus)	630	630	99%	0.0	100%	XP_002743193.1
<input type="checkbox"/> Chain A, Ah5 in Complex With 4-(4-(5,6-dimethyl-2-(2-pyridyl)-1H-pyridoxin-3,4,5-trimethoxyphenyl)pyridin-2-ylamino-2-amine	630	630	100%	0.0	100%	ZWOT_A
<input type="checkbox"/> PREDICTED: TGF-beta receptor type-1 like isoform X2 (Finnaeus europaeus)	630	630	99%	0.0	100%	XP_007524629.1
<input type="checkbox"/> PREDICTED: TGF-beta receptor type-1 isoform X2 (Papio anubis)	630	630	99%	0.0	100%	XP_003811500.1
<input type="checkbox"/> PREDICTED: TGF-beta receptor type-1 isoform X2 (Pan troglodytes)	630	630	99%	0.0	100%	XP_001159239.1
<input type="checkbox"/> PREDICTED: TGF-beta receptor type-1 isoform X2 (Macaca mulatta)	630	630	99%	0.0	100%	XP_001112621.1
<input type="checkbox"/> PREDICTED: TGF-beta receptor type-1 isoform X2 (Cavia porcellus)	630	630	99%	0.0	100%	XP_01308944.1
<input type="checkbox"/> PREDICTED: TGF-beta receptor type-1 isoform X2 (Mesocricetus auratus)	630	630	99%	0.0	100%	XP_005078788.2
<input type="checkbox"/> PREDICTED: TGF-beta receptor type-1 isoform X1 (Callithrix jacchus)	630	630	99%	0.0	100%	XP_009598388.1
<input type="checkbox"/> PREDICTED: TGF-beta receptor type-1 isoform X2 (Cercopithecus sabaeus)	630	630	99%	0.0	100%	XP_007666783.1
<input type="checkbox"/> PREDICTED: TGF-beta receptor type-1 isoform X1 (Cercopithecus sabaeus)	630	630	99%	0.0	100%	XP_007666782.1

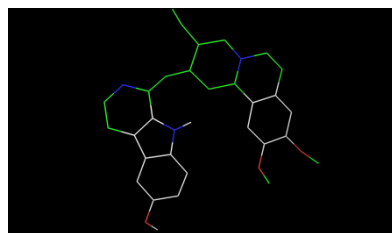
C

Figure 1: A. The ALK5 protein sequence; B. The 3D structure of ALK5 protein; C. The list of BLAST P of the protein sequence.

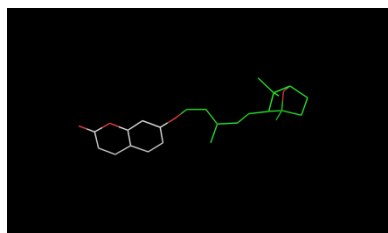
The stereochemical properties of the protein were assessed through a comprehensive analysis using the RAMPAGE Ramachandran plot. The results indicated that 98% of residues fell within the Favoured region (depicted in blue), with no residues in the Disallowed region (represented in white) (Figure 3).

Regarding the Absorption, Distribution, Metabolism, and

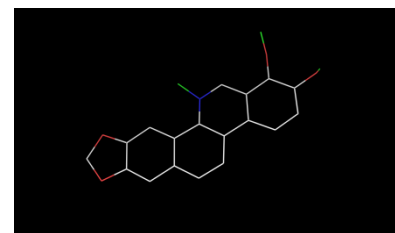
Excretion (ADME) of the thirteen ligands tested, the SwissADME website was employed for evaluation. Table 1 contains the ligands downloaded from PubChem, all of which conform to Lipinski's rule of five criteria: molecular mass below <500 g/mol, MLOGP values <5, the number of hydrogen acceptor chains <10, and the quantity of hydrogen donor chains <5.



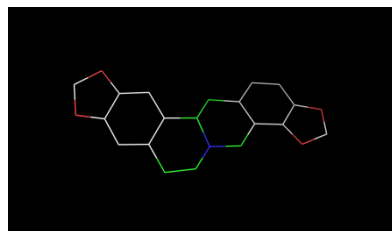
Tubulosine



Farnesiferol C



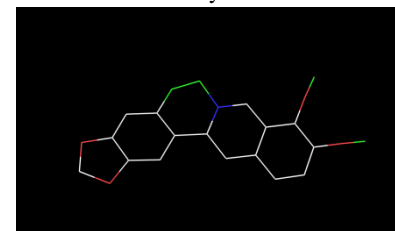
Chelerythrine



Stylophine



Sanguinarine



Berberine

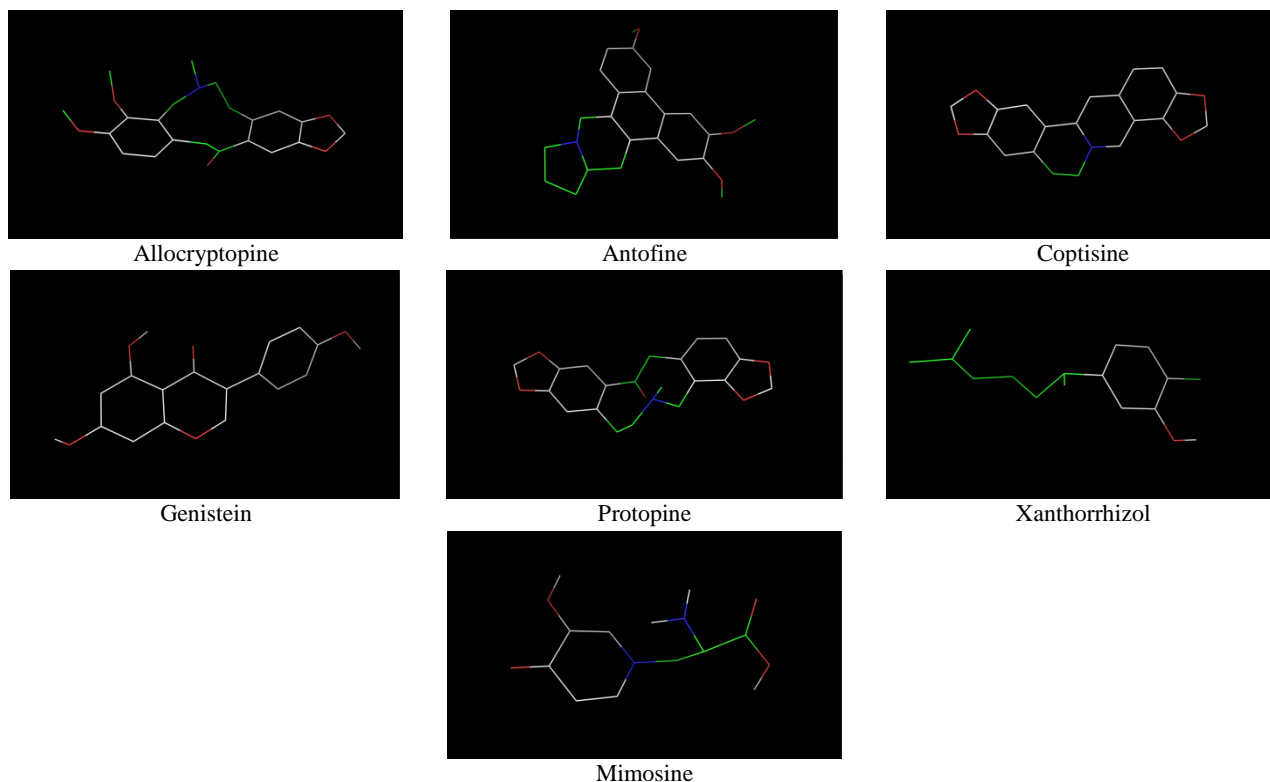
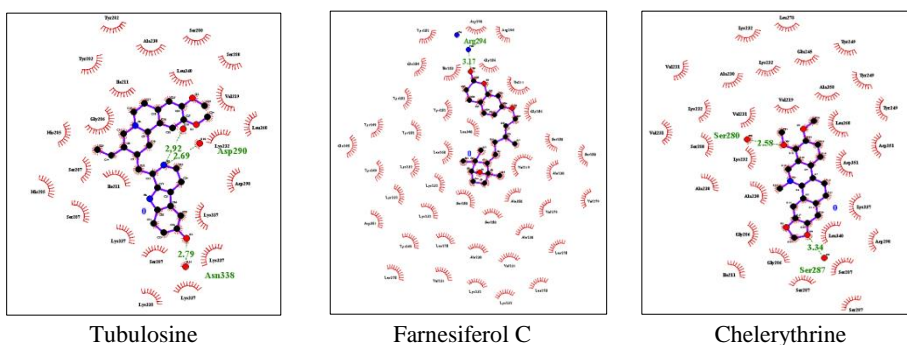


Figure 2: Ligand conformation results from molecular docking.

All ligands exhibiting high scores in the BOILED-Egg tests demonstrated significant GI absorption values. Additionally, the bioavailability (F) for these ligands was reasonably good, with more than 10% achieving a 55% rate. Once the ligands were confirmed to meet the necessary requirements, Autodock Tools were utilized to generate a protein devoid of water molecules. This allowed the protein and ligands to be transformed into .pdbqt format for subsequent analysis.

The analysis involved a grid box AGFR, which functions as a graphical user interface for defining the receptor docking grid box tailored for Autodock. Optionally, this process enabled the specification of a flexible side chain receptor for further investigation. The 2D and 3D interactions of the complex between the ALK5 protein and the ligand inhibitors are shown in Figure 3 and Figure 4, respectively.



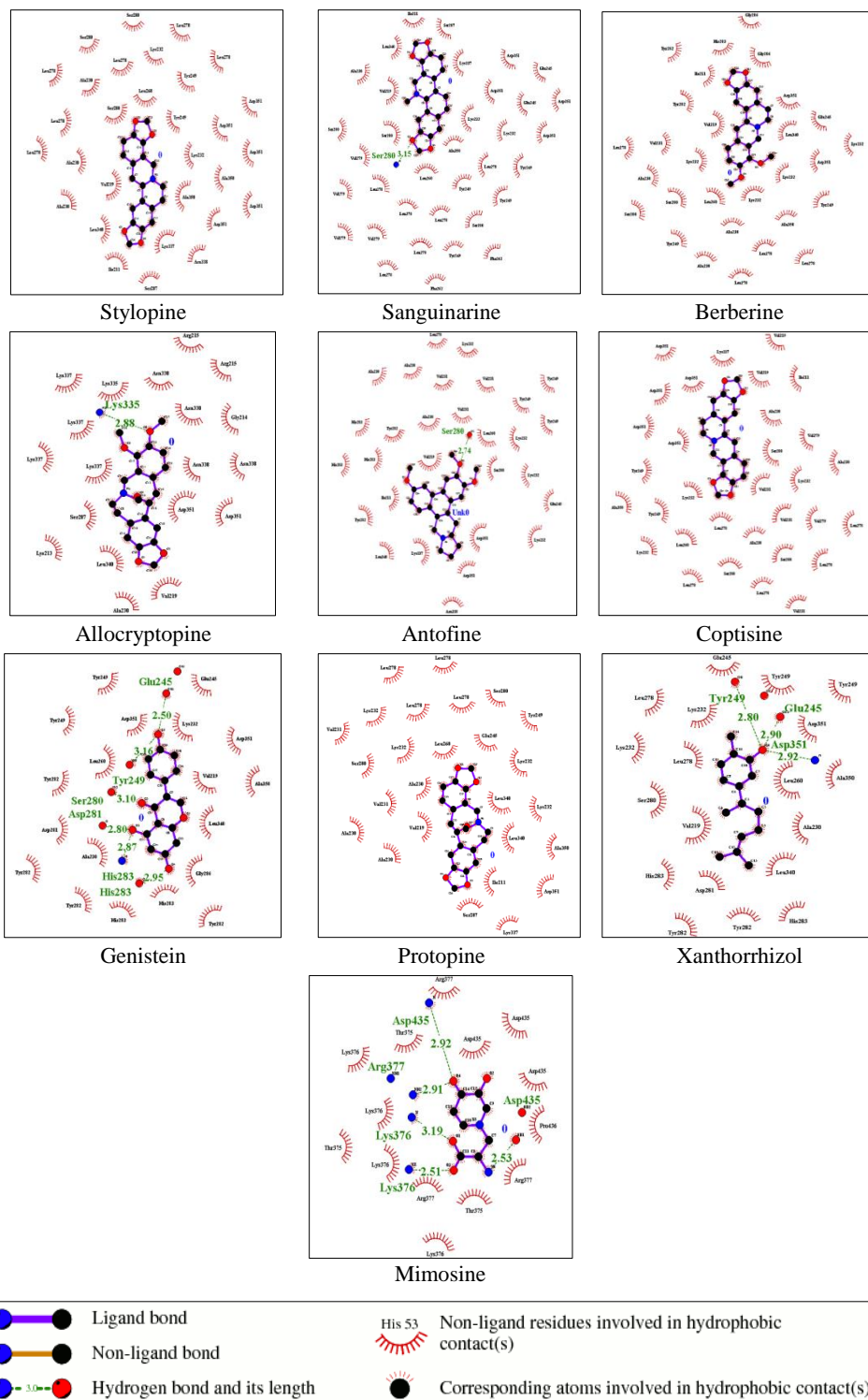


Figure 3: The 2D visualization of interactions complex between ALK5 receptor and the ligand inhibitors.

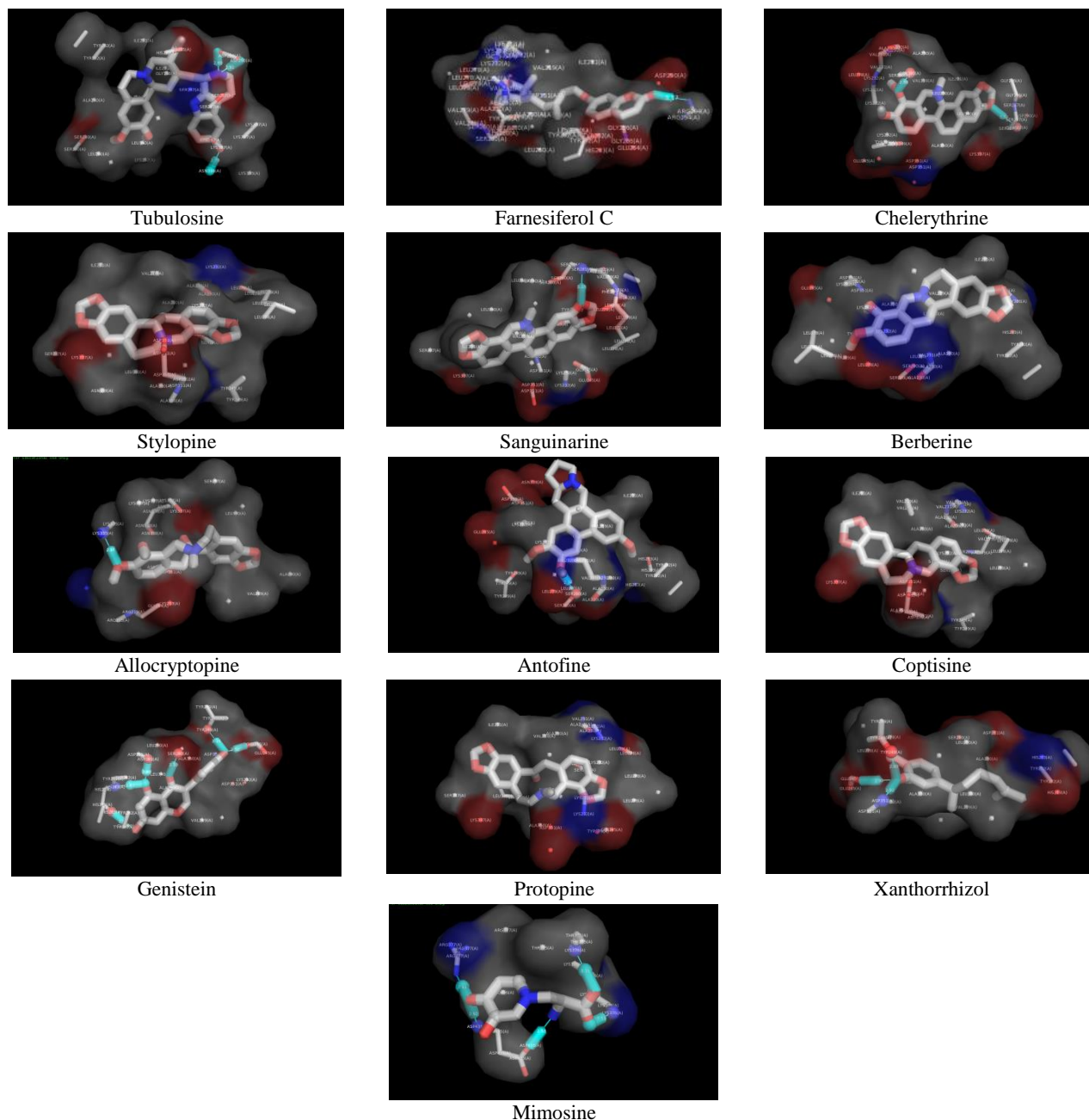


Figure 4: The 3D visualization of interactions complex between ALK5 receptor and the ligand inhibitors.

DISCUSSION

In the preparation process with AGFR, the attachment locations of ligands to the protein were determined based on the highest AS scores. The AS score represents the AutoSite value, indicating a high affinity for ligand binding pockets. The results from AGFR were saved in a .zip file format, containing a map for docking analysis that would be further processed using ADFR. The 3D schematic representation of the ligand conformations obtained from ADFR results for the 13 ligands, including tubulosine, farnesiferol c, chelerythrine,

stylophine, sanguinarine, berberine, allocryptopine, antofine, coptisine, genistein, protopine, xanthorrhizol, and mimosine, can be observed in figure 4. additionally, the ADFR analysis generated ligands in .pdbqt format, highlighting the most excellent ligand conformations, according to ADFR, capable of binding perfectly to the protein ALK5.

Furthermore, ADFR was performed on a commercial drug for NSCLC called carboplatin, which resulted in a ΔG value of -7.218 kcal/mol, smaller than the best ligand docking result,

Farnesiferol C ($\Delta G = -10.929$ kcal/mol). The ligand-protein complexes from ADFR results (Figure 2) were used for 2D and 3D representations using PyMOL, and the interaction between the protein and ligands was analyzed using LigPlot. The analysis involved hydrogen chains formed by residues, shown as dashed green lines, and hydrophobic bonds represented in red. The binding energy (ΔG) for each ligand obtained from ADFR indicated that the most negative score was the best result, as it implied stronger attraction energy between the protein and hydrophobic ligands on the target protein's surface.

Regarding the docking results for the receptor's flexibility, the best ΔG values were achieved by farnesiferol c (-10.929 kcal/mol), followed by tubulosine (-9.451 kcal/mol), genistein (-8.999 kcal/mol), xanthorrhizol (-8.641 kcal/mol), berberine (-8.411 kcal/mol), chelerythrine (-8.398 kcal/mol), mimosine (-8.392 kcal/mol), antofine (-8.349 kcal/mol), coptisine (-7.995 kcal/mol), sanguinarine (-7.993 kcal/mol), stylopine (-7.792 kcal/mol), protopine (-7.649 kcal/mol), and allocryptopine (-7.391 kcal/mol). LigPlot analysis (Figure 3) revealed that farnesiferol c formed a single hydrogen bond with Arg294 of the ALK5 protein structure. Tubulosine, the second-best ligand, created three hydrogen bonds in the binding pockets of ALK5 involving Asp290 and Asn338. Genistein, the third-ranked ligand, formed six hydrogen bonds with Glu245, Tyr249, Ser280, Asp281, and His283. The calculation of K_i (inhibition constant) showed that smaller ΔG values corresponded to lower K_i values, indicating a higher-quality ligand with the potential for blocking disease-causing proteins. Compared to the commercial drug carboplatin, which can cause side effects such as vomiting, hair loss, fatigue, and abnormal blood test results [28]. Research on mice has demonstrated that farnesiferol c, an anti-cancer drug, does not produce such side effects [29].

CONCLUSION

This study conducted a successful computational screening of 13 compounds derived from plants and one commercial drug to identify potential drug candidates for treating NSCLC. Molecular docking, a necessary molecular biology and drug design tool, was employed for the computational analysis. The screening involved the docking of these 13 ligands and the commercial drug from the PubChem database to the ALK5 protein, which is known to be overexpressed in lung cancer patients. The docking simulations were performed using Autodock for Flexible Receptors (ADFR), generating valuable data on the protein-ligand interactions between ALK5 and the 13 bioactive compounds. The *in silico* research revealed that farnesiferol C, a compound found in *Ferula assafoetida*, exhibited the most potent inhibition of the ALK5 protein, with a ΔG value lower than the commercial drug and the other 12 ligands. Consequently, farnesiferol C has the potential to be considered a promising drug candidate for treating NSCLC. However, further *in vitro* analysis is necessary to validate ALK5 as a target for lung cancer treatment using farnesiferol c and to explore its potential in the future.

ACKNOWLEDGEMENT

We would like to thank the Institute for Research and Community Development Unika Atma Jaya, the Directorate of Research and Development UI, and the Institute for Research and Community Service Unas for their continuous support.

REFERENCES

1. Sainz de Aja, J.; Dost, A.; Kim, C., Alveolar progenitor cells and the origin of lung cancer. *Journal of Internal Medicine* 2021, 289, 629-635.
2. Xie, Y.; Xue, C.; Guo, S.; Yang, L., MicroRNA-520a suppresses pathogenesis and progression of non-small-cell lung cancer through targeting the RRM2/Wnt axis. *Analytical Cellular Pathology* 2021, 2021.
3. Corrales, L.; Rosell, R.; Cardona, A. F.; Martin, C.; Zatarain-Barron, Z. L.; Arrieta, O., Lung cancer in never smokers: The role of different risk factors other than tobacco smoking. *Critical Reviews in Oncology/Hematology* 2020, 148, 102895.
4. Barta, J. A.; Powell, C. A.; Wisnivesky, J. P., Global epidemiology of lung cancer. *Annals of Global Health* 2019, 85.
5. Kushi, L. H.; Byers, T.; Doyle, C.; Bandera, E. V.; McCullough, M.; Gansler, T.; Andrews, K. S.; Thun, M. J., American Cancer Society Guidelines on Nutrition and Physical Activity for cancer prevention: reducing the risk of cancer with healthy food choices and physical activity. *CA: a Cancer Journal for Clinicians* 2006, 56, 254-281.
6. Calle, E. E.; Thun, M. J., Obesity and cancer. *Oncogene* 2004, 23, 6365-6378.
7. Boffetta, P., Human cancer from environmental pollutants: the epidemiological evidence. *Mutation Research/Genetic Toxicology and Environmental Mutagenesis* 2006, 608, 157-162.
8. Turner, M. C.; Andersen, Z. J.; Baccarelli, A.; Diver, W. R.; Gapstur, S. M.; Pope III, C. A.; Prada, D.; Samet, J.; Thurston, G.; Cohen, A., Outdoor air pollution and cancer: An overview of the current evidence and public health recommendations. *CA: a Cancer Journal for Clinicians* 2020, 70, 460-479.
9. Hensley, C. P.; Emerson, A. J., Non-Small Cell Lung Carcinoma: Clinical Reasoning in the Management of a Patient Referred to Physical Therapy for Costochondritis. *Physical Therapy* 2018, 98, 503-509.
10. Polański, J.; Chabowski, M.; Świątoniowska-Lonc, N.; Jankowska-Polańska, B.; Mazur, G., Can life satisfaction be considered a predictor of quality of life in patients with lung cancer? *European Review for Medical & Pharmacological Sciences* 2020, 24.
11. Liu, T.-C.; Jin, X.; Wang, Y.; Wang, K., Role of epidermal growth factor receptor in lung cancer and targeted therapies. *American Journal of Cancer Research* 2017, 7, 187.
12. Demaria, M.; O'Leary, M. N.; Chang, J.; Shao, L.; Liu, S.; Alimirah, F.; Koenig, K.; Le, C.; Mitin, N.; Deal, A. M., Cellular senescence promotes adverse effects of

- chemotherapy and cancer relapse. *Cancer Discovery* 2017, 7, 165-176.
13. Usui-Kawanishi, F.; Takahashi, M.; Sakai, H.; Suto, W.; Kai, Y.; Chiba, Y.; Hiraishi, K.; Kurahara, L. H.; Hori, M.; Inoue, R., Implications of immune-inflammatory responses in smooth muscle dysfunction and disease. *Journal of Smooth Muscle Research* 2019, 55, 81-107.
 14. Levy, L.; Hill, C. S., Alterations in components of the TGF- β superfamily signaling pathways in human cancer. *Cytokine & Growth Factor Reviews* 2006, 17, 41-58.
 15. Syed, V., TGF- β signaling in cancer. *Journal of Cellular Biochemistry* 2016, 117, 1279-1287.
 16. Wrzesinski, S. H.; Wan, Y. Y.; Flavell, R. A., Transforming growth factor- β and the immune response: implications for anticancer therapy. *Clinical Cancer Research* 2007, 13, 5262-5270.
 17. Kim, B.-G.; Malek, E.; Choi, S. H.; Ignatz-Hoover, J. J.; Driscoll, J. J., Novel therapies emerging in oncology to target the TGF- β pathway. *Journal of Hematology & Oncology* 2021, 14, 1-20.
 18. Sisodiya, P. S., Plant derived anticancer agents: a review. *Int. J. Res. Dev. Pharm. Life Sci* 2013, 2, 293-308.
 19. Istudor, V., Pharmacologically active natural compounds for lung cancer. *Alternative Medicine Review* 2004, 9, 402-419.
 20. Lee, J.-H.; Choi, S.; Lee, Y.; Lee, H.-J.; Kim, K.-H.; Ahn, K.-S.; Bae, H.; Lee, H.-J.; Lee, E.-O.; Ahn, K.-S., Herbal compound farnesiferol C exerts antiangiogenic and antitumor activity and targets multiple aspects of VEGFR1 (Flt1) or VEGFR2 (Flk1) signaling cascades. *Molecular Cancer Therapeutics* 2010, 9, 389-399.
 21. Misiurek, J.; Plech, T.; Kaproń, B.; Makuch-Kocka, A.; Szultka-Młyńska, M.; Buszewski, B.; Petruczynik, A., Determination of Some Isoquinoline Alkaloids in Extracts Obtained from Selected Plants of the Ranunculaceae, Papaveraceae and Fumarioideae Families by Liquid Chromatography and In Vitro and In Vivo Investigations of Their Cytotoxic Activity. *Molecules* 2023, 28, 3503.
 22. Nagaraju, G. P.; Zafar, S. F.; El-Rayes, B. F., Pleiotropic effects of genistein in metabolic, inflammatory, and malignant diseases. *Nutrition Reviews* 2013, 71, 562-572.
 23. Kwan, Y.; Su, T.; Fu, X.; Tse, A.; Fong, W. F.; Yu, Z. L., Herbal remedies against adipogenesis. *Journal of Alternative Medical Research* 2015, 1, 1-7.
 24. Simamora, A.; Timotius, K. H.; Yerer, M. B.; Setiawan, H.; Mun'im, A., Xanthorrhizol, a potential anticancer agent, from *Curcuma xanthorrhiza* Roxb. *Phytomedicine* 2022, 154359.
 25. Norfadhilah, R. Extraction of mimosine from dried leaves and defatted seed of *Leucaena leucocephala* and its biodiesel oxidative stability/Norfadhilah Ramli. University of Malaya, 2019.
 26. Heinzelmann, G.; Gilson, M. K., Automation of absolute protein-ligand binding free energy calculations for docking refinement and compound evaluation. *Scientific Reports* 2021, 11, 1116.
 27. Vilar, S.; Sobarzo-Sanchez, E.; Santana, L.; Uriarte, E., Molecular docking and drug discovery in β -adrenergic receptors. *Current Medicinal Chemistry* 2017, 24, 4340-4359.
 28. Hsu, H.-C.; Tsai, S.-Y.; Wu, S.-L.; Jeang, S.-R.; Ho, M.-Y.; Liou, W.-S.; Chiang, A.-J.; Chang, T.-H., Longitudinal perceptions of the side effects of chemotherapy in patients with gynecological cancer. *Supportive Care in Cancer* 2017, 25, 3457-3464.
 29. Davatgaran-Taghipour, Y.; Masoomzadeh, S.; Farzaei, M. H.; Bahramsoltani, R.; Karimi-Soureh, Z.; Rahimi, R.; Abdollahi, M., Polyphenol nanoformulations for cancer therapy: experimental evidence and clinical perspective. *International Journal of Nanomedicine* 2017, 2689-2702.